

ANTI-DIFFUSIVE FINITE DIFFERENCE WENO METHODS FOR SHALLOW WATER WITH TRANSPORT OF POLLUTANT ^{*1)}

Zhengfu Xu

(Department of Mathematics, Pennsylvania State University, University Park, PA 16802, USA)

Chi-Wang Shu

(Division of Applied Mathematics, Brown University, Providence, Rhode Island 02912, USA)

Dedicated to the 70th birthday of Professor Lin Qun

Abstract

In this paper we further explore and apply our recent anti-diffusive flux corrected high order finite difference WENO schemes for conservation laws [18] to compute the Saint-Venant system of shallow water equations with pollutant propagation, which is described by a transport equation. The motivation is that the high order anti-diffusive WENO scheme for conservation laws produces sharp resolution of contact discontinuities while keeping high order accuracy for the approximation in the smooth region of the solution. The application of the anti-diffusive high order WENO scheme to the Saint-Venant system of shallow water equations with transport of pollutant achieves high resolution

Mathematics subject classification: 65M06, 76B15.

Key words: Anti-diffusive flux correction, Sharpening contact discontinuity, High order accuracy, Finite difference WENO scheme, Saint-Venant system of shallow water, Transport of pollutant.

1. Introduction

In this paper, we are interested in computing the transport of a passive pollutant in the flow modeled by the Saint-Venant system, given in the one dimensional case by

$$\begin{cases} h_t + (hu)_x = S \\ (hu)_t + (hu^2 + \frac{gh^2}{2})_x = -ghB_x \end{cases} \quad (1.1)$$

which is introduced in [16] and regularly used as a simplified model to describe shallow water flows. Here h is the depth, u is the velocity of water, g is the gravity constant, S is the pollutant source term, and $B(x)$ is the bottom topography. We are interested in locating the exact position and the correct concentration of the pollutant which is decided by a transport equation

$$(hT)_t + (uhT)_x = T_s S \quad (1.2)$$

where T is the pollutant concentration, and T_s is the concentration of the pollutant at the source. This model is used for the computation in [3] with a finite-volume particle (FVP) method. The FVP method is a hybrid method as a combination of two methods. For the

* Received March 1, 2006.

¹⁾Research supported by ARO grant W911NF-04-1-0291 and NSF grant DMS-0510345.

shallow water equation (1.1), the finite volume method is used, and for the transport equation (1.2), the particle method is deployed. In [3], the authors also applied filters on the FVP method to smooth out the oscillations introduced by a combination of two different mechanisms.

The equation (1.2), which describes the transport of pollutant, is a linear equation for the variable hT for a given velocity u , thus the solution involving the pollutant will contain a contact discontinuity when initially hT is discontinuous. To locate the exact location and concentration of the pollutant, we need to resolve well the contact discontinuity in the solution, which is a difficult task as contact discontinuities, unlike shocks, are easily smeared by a shock capturing numerical method. There have been a lot of efforts in the literature to overcome the problem of the smearing of contact discontinuities. We refer, e.g., to [5, 6, 19] and the references therein.

Recently, Després and Lagoutière [4] proposed a new approach called limited downwind scheme, much akin to a class of flux limiters by Sweby [17], to prevent the smearing of contact discontinuities while keeping nonlinear stability. Their scheme is identical with the Superbee scheme developed by Roe [11] in the case of linear advection. By introducing an anti-diffusive flux, it gives remarkably sharp profiles of contact discontinuities in both one dimensional scalar and system cases. More importantly, they observe numerically and prove theoretically that their scheme adopts a class of *moving* traveling wave solutions exactly. This has an important implication that the smearing of contact discontinuities will not be progressively more severe for longer time, but will be stabilized for all time. A later paper by Bouchut [1] further modifies this scheme to satisfy entropy conditions and also gives a simple explicit formula for this limited downwind anti-diffusive flux.

In [18], we generalized the downwind flux correction idea to two dimensions and we developed a class of anti-diffusive high order finite difference WENO schemes to resolve contact discontinuities for conservation law equations. By going to high order accuracy, we were able to remove the unpleasant stairs in smooth regions when a first order anti-diffusive scheme is used. Ample numerical results in [18] indicate that our scheme can resolve well the contact discontinuities and at the same time maintains the stability and accuracy of regular high order WENO schemes for shocks and smooth structures of the solution. In this paper, we would like to further explore and apply the high order anti-diffusive finite difference WENO schemes in [18] to solve the equations (1.1) and (1.2) as a system, with the objective of obtaining sharp resolution of the contact discontinuities of the pollutant propagation.

High order finite difference WENO schemes in [9] were developed based on the successful ENO schemes [7, 14, 15] and third order finite volume WENO schemes [10], and have been quite successful in computational fluid dynamics and other applications. They are especially suitable for problems containing both shocks and complicated smooth flow features. For more details, we refer to the lecture notes [12] and the survey paper [13], and the references therein.

This paper is organized as follows. In Section 2 we briefly review the anti-diffusive high order finite difference WENO schemes in [18] with improved non-smoothness indicators. In Section 3 we apply this anti-diffusive finite difference scheme on the system (1.1) and (1.2) and give numerical results. In Section 4 we apply the anti-diffusive finite difference scheme on two dimensional models and show the success of the application through typical numerical tests. Concluding remarks are given in Section 5.

2. Flux Corrections for High Order Finite Difference WENO Schemes for Conservation Laws

In this section, we briefly review the techniques developed and applied in [18] for the conservation law equation

$$u_t + f(u)_x = 0 \tag{2.1}$$

with the assumption $f'(u) > 0$, for simplicity. The scheme for the other case $f'(u) < 0$ can be

designed symmetrically.

2.1. Flux Correction for Finite Difference WENO Schemes

We will present the high order flux correction technique in [18] by third order TVD Runge-Kutta in time and fifth order finite difference WENO reconstruction in space. The full discretization has the following form

$$\begin{aligned} u^{(1)} &= u^n + \Delta t L(u^n) \\ u^{(2)} &= u^n + \frac{1}{4} \Delta t L'(u^n) + \frac{1}{4} \Delta t L(u^{(1)}) \\ u^{n+1} &= u^n + \frac{1}{6} \Delta t L''(u^n) + \frac{1}{6} \Delta t L(u^{(1)}) + \frac{2}{3} \Delta t L(u^{(2)}) \end{aligned} \quad (2.2)$$

where, on a uniform grid $x_i = i\Delta x$ (for simplicity of presentation), u_i denotes the point value at x_i and the operator L is defined by

$$L(u)_i = -\lambda_i \left(\hat{f}_{i+\frac{1}{2}}^a - \hat{f}_{i-\frac{1}{2}}^a \right) \quad (2.3)$$

with $\lambda_i = \frac{\Delta t}{\Delta x_i}$ (for the uniform mesh case under consideration $\Delta x_i = \Delta x$) and the anti-diffusive flux \hat{f}^a given by

$$\hat{f}_{i+\frac{1}{2}}^a = f_{i+\frac{1}{2}}^- + \varphi_i \min\text{mod} \left(\frac{u_i - u_{i-1}}{\lambda_i} + f_{i-\frac{1}{2}}^- - f_{i+\frac{1}{2}}^-, f_{i+\frac{1}{2}}^+ - f_{i+\frac{1}{2}}^- \right)$$

where $f_{i+\frac{1}{2}}^-$ and $f_{i+\frac{1}{2}}^+$ are the fifth order WENO fluxes based on left-biased upwinding and right-biased upwinding, respectively, see [9] for details. The cost of the computation for the anti-diffusive flux \hat{f}^a is about the same as that for a regular WENO-LF flux, again see [9]. The purpose for the introduction of the operators L' and L'' in (2.2) in [18] is to maintain the moving traveling wave solutions for piecewise constant functions. The operator L' is defined by

$$L'(u)_i = -\lambda_i \left(\bar{f}_{i+\frac{1}{2}}^a - \bar{f}_{i-\frac{1}{2}}^a \right) \quad (2.4)$$

with the modified anti-diffusive flux \bar{f}^a given by

$$\bar{f}_{i+\frac{1}{2}}^a = \begin{cases} f_{i+\frac{1}{2}}^- + \varphi_i \min\text{mod} \left(\frac{4(u_i - u_{i-1})}{\lambda_i} + f_{i-\frac{1}{2}}^- - f_{i+\frac{1}{2}}^-, f_{i+\frac{1}{2}}^+ - f_{i+\frac{1}{2}}^- \right) \\ \hat{f}_{i+\frac{1}{2}}^a \end{cases}$$

corresponding to cases

$$\begin{cases} bc > 0, & |b| < |c| \\ \text{otherwise} \end{cases}$$

respectively. The operator L'' is defined by

$$L''(u)_i = -\lambda_i \left(\tilde{f}_{i+\frac{1}{2}}^a - \tilde{f}_{i-\frac{1}{2}}^a \right) \quad (2.5)$$

with the modified anti-diffusive flux \tilde{f}^a given by

$$\tilde{f}_{i+\frac{1}{2}}^a = \begin{cases} f_{i+\frac{1}{2}}^- + \varphi_i \min\text{mod} \left(\frac{6(u_i - u_{i-1})}{\lambda_i} + f_{i-\frac{1}{2}}^- - f_{i+\frac{1}{2}}^-, f_{i+\frac{1}{2}}^+ - f_{i+\frac{1}{2}}^- \right) \\ \hat{f}_{i+\frac{1}{2}}^a \end{cases}$$

corresponding to cases

$$\begin{cases} bc > 0, & |b| < |c| \\ \text{otherwise} \end{cases}$$

respectively. Here b, c are defined as $b = \frac{u_i - u_{i-1}}{\lambda_i} + f_{i-\frac{1}{2}}^- - f_{i+\frac{1}{2}}^-$, $c = f_{i+\frac{1}{2}}^+ - f_{i+\frac{1}{2}}^-$ and φ_i is a discontinuity indicator between 0 and 1. Ideally, φ_i should be close to 0 in smooth regions and close to 1 near a discontinuity. We refer to [18] for our original choice of φ_i and we describe a somewhat improved choice in Section 2.2. We remark that the scheme (2.2), with L, L' and L'' defined by (2.3), (2.4) and (2.5) respectively, is fifth order accurate in space and third order accurate in time. The correction to the original WENO is no larger in magnitude than that of $f_{i+\frac{1}{2}}^+ - f_{i+\frac{1}{2}}^-$, which is on the level of truncation errors for the WENO schemes because both $f_{i+\frac{1}{2}}^+$ and $f_{i+\frac{1}{2}}^-$ are high order approximations to the same flux at the same location. This ensures that the high order accuracy of the finite difference WENO schemes is maintained. The purpose of the extra factor 4 in the first argument of the minmod function in the definition of \tilde{f}^a and the extra factor 6 in the first argument of the minmod function in the definition of \tilde{f}^a is to compensate for the coefficients $\frac{1}{4}$ and $\frac{1}{6}$ in front of L' and L'' respectively, so that the final scheme could still maintain exactly traveling wave solutions of a piecewise constant function. We refer to [18] for more details and numerical experiments for this anti-diffusive flux-corrected WENO scheme, and to [9] for the details of the fifth order finite difference WENO reconstruction. For the WENO-Roe scheme in [9], the numerical flux is chosen as $f_{i+\frac{1}{2}}^-$ when $f'(u) > 0$ and as $f_{i+\frac{1}{2}}^+$ when $f'(u) \leq 0$. Therefore, the anti-diffusive flux-corrected WENO scheme is a flux correction to the WENO-Roe scheme. Because WENO-Roe scheme may violate entropy conditions without an entropy correction, we only apply the anti-diffusive flux-correction on linear problems or for linearly degenerate fields in systems.

2.2. The Discontinuity Indicator

The discontinuity indicator φ_i was designed in [18] such that it is close to 0 in smooth regions and close to 1 near a discontinuity. Out of consideration for symmetry and somewhat better numerical performance, we improve the definition of φ_i to the following form:

$$\varphi_i = \frac{\beta_i}{\beta_i + \gamma_i} \tag{2.6}$$

where

$$\alpha_i = |u_{i-1} - u_i|^2 + \varepsilon, \quad \xi_i = |u_{i-1} - u_{i+1}|^2 + \varepsilon, \quad \beta_i = \frac{\xi_i}{\alpha_{i-1}} + \frac{\xi_i}{\alpha_{i+2}}, \quad \gamma_i = \frac{|u_{\max} - u_{\min}|^2}{\alpha_i}. \tag{2.7}$$

Here ε is a small positive number taken as 10^{-6} in our numerical experiments, and u_{\max} and u_{\min} are the maximum and minimum values of u_j for all cells. Clearly, $0 \leq \varphi_i \leq 1$, and $\varphi_i = O(\Delta x^2)$ in smooth regions. Near a strong discontinuity, $\gamma_i \ll \beta_i$, φ_i is close to 1.

2.3. Flux Corrections for the Finite Difference WENO Schemes in Two Dimensions

Two dimensional finite difference WENO schemes are similar to the schemes for one dimension, with reconstruction computed in each direction. Thus, after reconstruction of $f_{i+\frac{1}{2},j}^-$, $f_{i+\frac{1}{2},j}^+$, $f_{i,j+\frac{1}{2}}^-$, $f_{i,j+\frac{1}{2}}^+$ at interfaces between cells from given point values $f_{i,j}$, for the equation

$$u_t + f(u)_x + g(u)_y = 0, \quad f' > 0, \quad g' > 0, \tag{2.8}$$

we present the anti-diffusive flux by

$$\begin{aligned}\hat{f}_{i+\frac{1}{2},j}^a &= f_{i+\frac{1}{2},j}^- \\ &+ \varphi_{i,j} \min\text{mod} \left(\frac{u_{i,j} - u_{i-1,j}}{d\lambda_{i,j}^x} + f_{i-\frac{1}{2},j}^- - f_{i+\frac{1}{2},j}^-, f_{i+\frac{1}{2},j}^+ - f_{i+\frac{1}{2},j}^- \right)\end{aligned}$$

where $d = 2$ is the dimension. For fixed j , $\varphi_{i,j}$ has the same definition as in Section 2.2 in one dimension. Symmetrically, in the y direction, we have

$$\begin{aligned}\hat{g}_{i,j+\frac{1}{2}}^a &= g_{i,j+\frac{1}{2}}^- \\ &+ \psi_{i,j} \min\text{mod} \left(\frac{u_{i,j} - u_{i,j-1}}{d\lambda_{i,j}^y} + g_{i,j-\frac{1}{2}}^- - g_{i,j+\frac{1}{2}}^-, g_{i,j+\frac{1}{2}}^+ - g_{i,j+\frac{1}{2}}^- \right)\end{aligned}$$

with the discontinuity indicator $\psi_{i,j}$ defined similarly to the one dimensional case in Section 2.2 in the y direction with fixed x_i .

We use the third order TVD Runge-Kutta method for the time discretization. Two dimensional systems are treated dimension by dimension, with anti-diffusive flux in each dimension defined as above.

3. Computation of Saint-Venant Equations with Transport of Pollutant in One Dimension

In this section, we apply the algorithm described in the last section to the combined system

$$\begin{cases} h_t + (hu)_x = S, \\ (hu)_t + (hu^2 + \frac{gh^2}{2})_x = -ghB_x \\ (hT)_t + (u hT)_x = T_s S. \end{cases} \quad (3.1)$$

3.1. Characteristic Decomposition

A brief computation of (3.1) gives the following Jacobian

$$J = \begin{pmatrix} 0 & 1 & 0 \\ gh - u^2 & 2u & 0 \\ -uT & T & u \end{pmatrix}.$$

The three eigenvalues of this Jacobian are $\lambda^{(1)} = u - \sqrt{gh}$, $\lambda^{(2)} = u + \sqrt{gh}$ and $\lambda^{(3)} = u$. The matrices composed of the three corresponding right and left eigenvectors are

$$R = \begin{pmatrix} 1 & 1 & 0 \\ u - \sqrt{gh} & u + \sqrt{gh} & 0 \\ T & T & 1 \end{pmatrix}$$

and

$$L = \begin{pmatrix} (u + \sqrt{gh}) \frac{0.5}{\sqrt{gh}} & -\frac{0.5}{\sqrt{gh}} & 0 \\ (\sqrt{gh} - u) \frac{0.5}{\sqrt{gh}} & \frac{0.5}{\sqrt{gh}} & 0 \\ -T & 0 & 1 \end{pmatrix}$$

respectively. We can easily check that $\frac{\partial \lambda^{(3)}}{\partial \mathbf{u}} \cdot R^{(3)} = 0$. Here $\mathbf{u} = (h, hu, hT)$ and $R^{(3)}$ is the right eigenvector corresponding to $\lambda^{(3)}$. Thus the third characteristic field is a linearly degenerate field. We refer to [12] for the details of the procedure for the characteristic decomposition

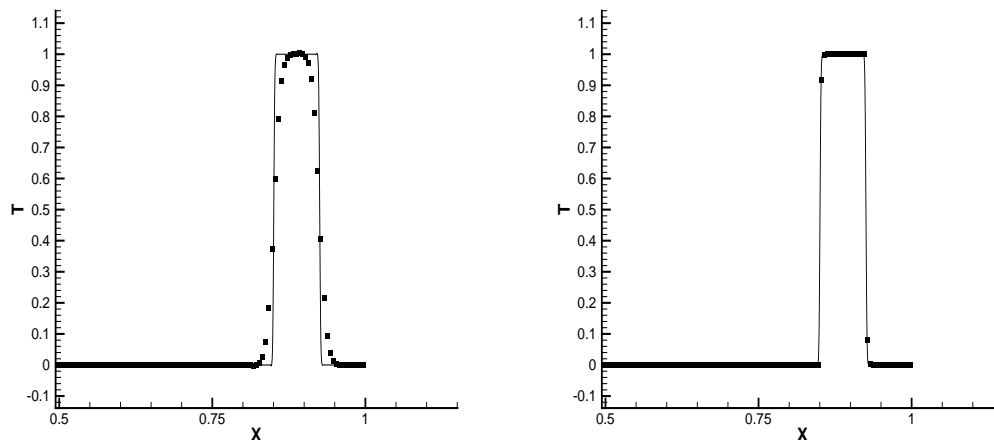


Figure 3.1: Example 3.2.1. 200 uniform mesh points. $t = 4$, $CFL = 0.3$. Solid lines: reference solution computed by the regular fifth order WENO scheme with 2000 mesh points; filled rectangles: numerical solution. Left: regular fifth order WENO; Right: anti-diffusive fifth order WENO.

with the fifth order finite difference WENO reconstruction. In the first and second genuinely nonlinear fields, we use the Lax-Friedrichs flux splitting, and in the third field, which is a linearly degenerate field, we apply the anti-diffusive flux.

3.2. Numerical Tests

In this subsection, we perform numerical experiment on two examples which are used in [3].

Example 3.2.1. Advection of pollutant. The setup is as follows: $h(x, 0) + B(x) = 1.0$, $h(x, 0)u(x, 0) = -0.1$, $g = 1$, $S = 0$, and the bottom topography is described by

$$B(x) = \begin{cases} 0.25(\cos(10\pi(x - 0.5)) + 1), & 0.4 \leq x \leq 0.6 \\ 0, & \text{otherwise} \end{cases} \quad (3.2)$$

The initial pollutant concentration is

$$T(x, 0) = \begin{cases} 1, & 0.4 \leq x \leq 0.5 \\ 0, & \text{otherwise} \end{cases} \quad (3.3)$$

The computational domain is $[0, 1]$ and this problem is run to $t = 4$. The numerical result in Figure 3.1 shows excellent resolution of the location and concentration of the pollutant by our anti-diffusive scheme.

Example 3.2.2. Dam Break. The initial condition is

$$(h, u, T) = \begin{cases} (1.0, 0, 0.7), & x < 0 \\ (0.5, 0, 0.5), & \text{otherwise} \end{cases} \quad (3.4)$$

with the gravitational constant $g = 9.8$, $S = 0$. The computational domain is $[-1, 1]$ and the scheme is run to $t = 0.24$. Again we observe sharp resolution of the location and concentration

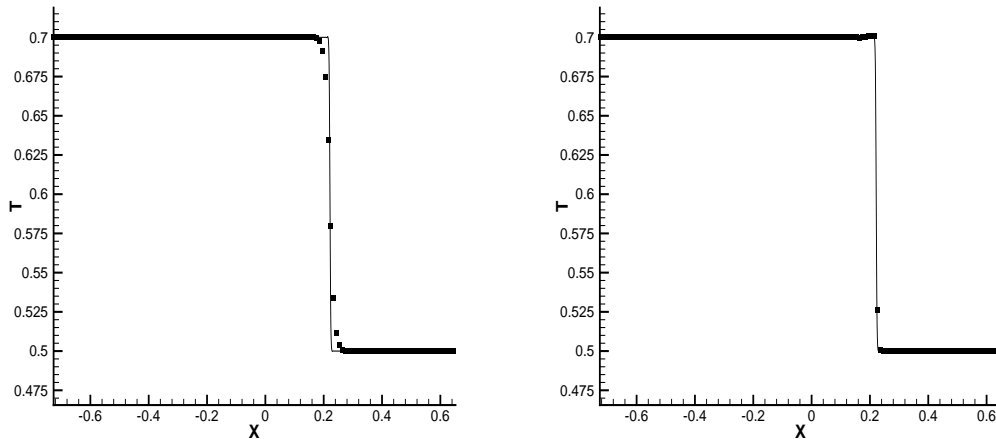


Figure 3.2: Example 3.2.2. 200 uniform mesh. $t = 0.24$, $CFL = 0.3$. Solid lines: reference solution computed by the regular fifth order WENO scheme with 2000 mesh points; filled rectangles: numerical solution. Left: regular fifth order WENO; Right: anti-diffusive fifth order WENO.

of the pollutant in Figure 3.2. Numerical results can be compared to those in [3] (module a scale by a factor of 1000).

4. Computation of the Saint-Venant Equations with Transport of Pollutant in Two Dimensions

In this section, we apply the algorithm to the two dimensional system

$$\begin{cases} h_t + (hu)_x + (hv)_y = S, \\ (hu)_t + (hu^2 + \frac{gh^2}{2})_x + (huv)_y = -ghB_x \\ (hv)_t + (huv)_x + (hv^2 + \frac{gh^2}{2})_y = -ghB_y \\ (hT)_t + (uhT)_x + (vhT)_y = T_s S. \end{cases} \quad (4.1)$$

4.1. Characteristic Decomposition

A brief computation of (4.1) gives the following Jacobians

$$J_x = \begin{pmatrix} 0 & 1 & 0 & 0 \\ gh - u^2 & 2u & 0 & 0 \\ -uv & v & u & 0 \\ -uT & T & 0 & u \end{pmatrix}$$

and

$$J_y = \begin{pmatrix} 0 & 0 & 1 & 0 \\ -uv & v & u & 0 \\ gh - v^2 & 0 & 2v & 0 \\ -vT & 0 & T & v \end{pmatrix}$$

in the x and y directions respectively.

The four eigenvalues of the Jacobian J_x are

$$\lambda^{(1)} = u - \sqrt{gh}, \quad \lambda^{(2)} = u + \sqrt{gh}, \quad \lambda^{(3)} = u, \quad \lambda^{(4)} = u.$$

The matrices composed of the four corresponding right and left eigenvectors are

$$R_x = \begin{pmatrix} 1 & 1 & 0 & 0 \\ u - \sqrt{gh} & u + \sqrt{gh} & 0 & 0 \\ v & v & 1 & 0 \\ T & T & 0 & 1 \end{pmatrix}$$

and

$$L_x = \begin{pmatrix} (u + \sqrt{gh}) \frac{0.5}{\sqrt{gh}} & -\frac{0.5}{\sqrt{gh}} & 0 & 0 \\ (\sqrt{gh} - u) \frac{0.5}{\sqrt{gh}} & \frac{0.5}{\sqrt{gh}} & 0 & 0 \\ -v & 0 & 1 & 0 \\ -T & 0 & 0 & 1 \end{pmatrix}$$

We can check easily that $\frac{\partial \lambda^{(i)}}{\partial \mathbf{u}} \cdot R^{(i)} = 0$ for $i = 3, 4$. Here $\mathbf{u} = (h, hu, hv, hT)$ and $R^{(i)}$ is the right eigenvector corresponding to $\lambda^{(i)}$. Thus the third and the fourth characteristic fields are linearly degenerate fields and we will use the anti-diffusive fluxes on these fields.

Similar computation in the y direction gives the following eigenvalues for the Jacobian J_y

$$\lambda^{(1)} = v - \sqrt{gh}, \quad \lambda^{(2)} = v + \sqrt{gh}, \quad \lambda^{(3)} = v, \quad \lambda^{(4)} = v.$$

The matrices composed of the four corresponding right and left eigenvectors are

$$R_y = \begin{pmatrix} 1 & 1 & 0 & 0 \\ u & u & 1 & 0 \\ v - \sqrt{gh} & v + \sqrt{gh} & 0 & 0 \\ T & T & 0 & 1 \end{pmatrix}$$

and

$$L_y = \begin{pmatrix} (v + \sqrt{gh}) \frac{0.5}{\sqrt{gh}} & 0 & -\frac{0.5}{\sqrt{gh}} & 0 \\ (\sqrt{gh} - v) \frac{0.5}{\sqrt{gh}} & 0 & \frac{0.5}{\sqrt{gh}} & 0 \\ -u & 1 & 0 & 0 \\ -T & 0 & 0 & 1 \end{pmatrix}$$

Once again we can check that $\frac{\partial \lambda^{(i)}}{\partial \mathbf{u}} \cdot R^{(i)} = 0$ for $i = 3, 4$. Thus the third and the fourth characteristic fields are linearly degenerate fields and we will use the anti-diffusive fluxes on these fields.

4.2. Numerical Tests

In this subsection, we perform numerical experiments using the anti-diffusive high order WENO schemes on the shallow water models involving the transport of pollutant in two dimensions.

Example 4.2.1. Partial dam break. This test case concerns a partial failure of a dam in a $200 \times 200 m^2$ basin. This problem has been computed by many authors (e.g. [2] and the references therein). We scale this problem by 100 and the setup is as follows: $h(x, y, 0) = 1.0$, $b(x, y) = 0$, $u(x, y, 0) = v(x, y, 0) = 0$, $T(x, y, 0) = 0.7$ when $x < 1.0$; $h(x, y, 0) = 0.3$, $b(x, y) = 0$, $u(x, y, 0) = v(x, y, 0) = 0$, $T(x, y, 0) = 0.2$ when $x \geq 1.0$; $g = 9.8$, $S = 0$. The computational domain is $[0, 2] \times [0, 2]$ and the break is located at $x = 1.0$, between $y = 0.7$ and $y = 1.3$. We run the computation on this problem to $t = 0.2$ with $CFL = 0.3$. The numerical results in Figures

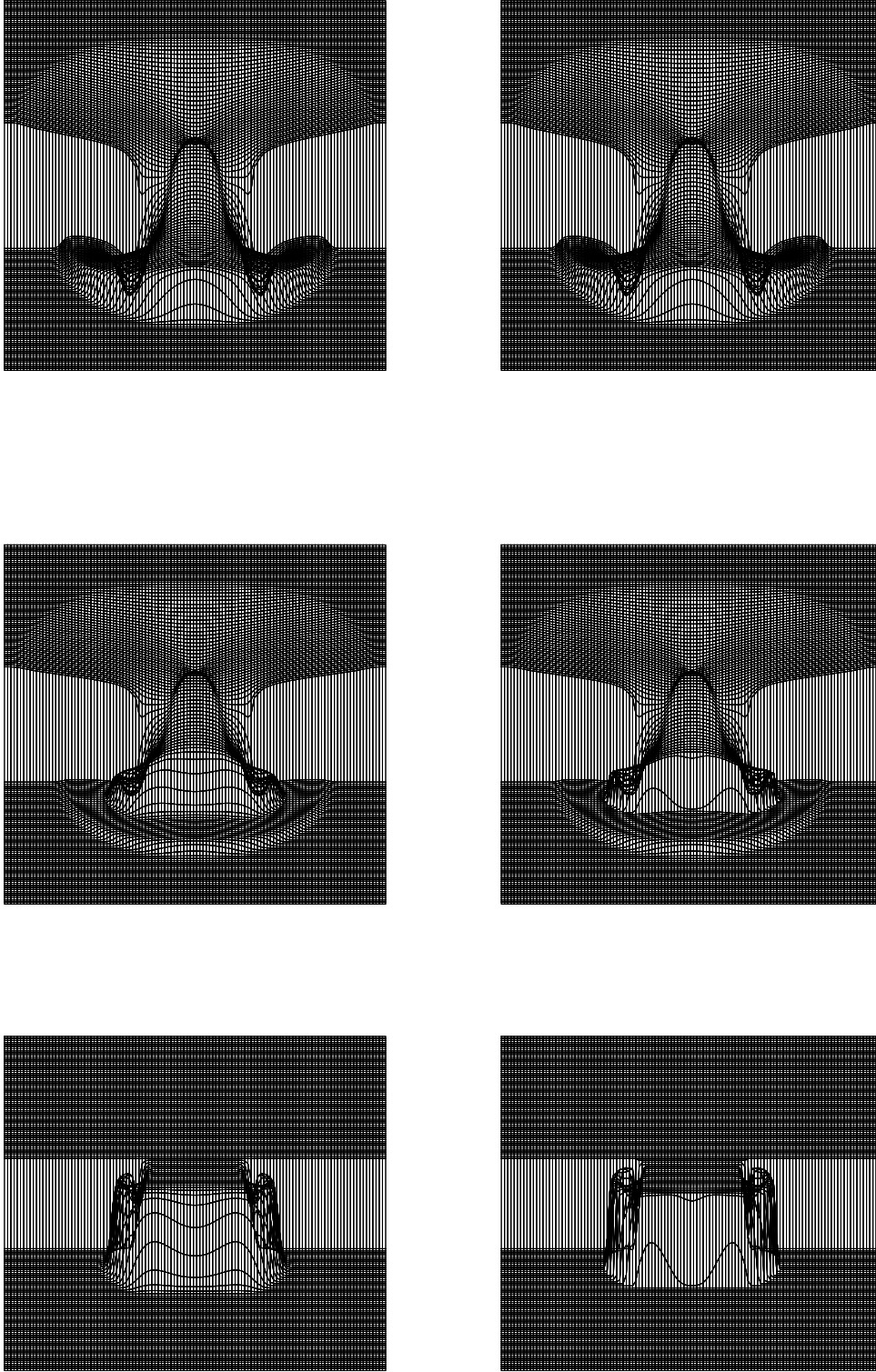


Figure 4.1: Example 4.2.1. 120×120 uniform mesh. From top to bottom: surfaces of h , hT and T . Left: regular fifth order WENO; Right: anti-diffusive fifth order WENO.

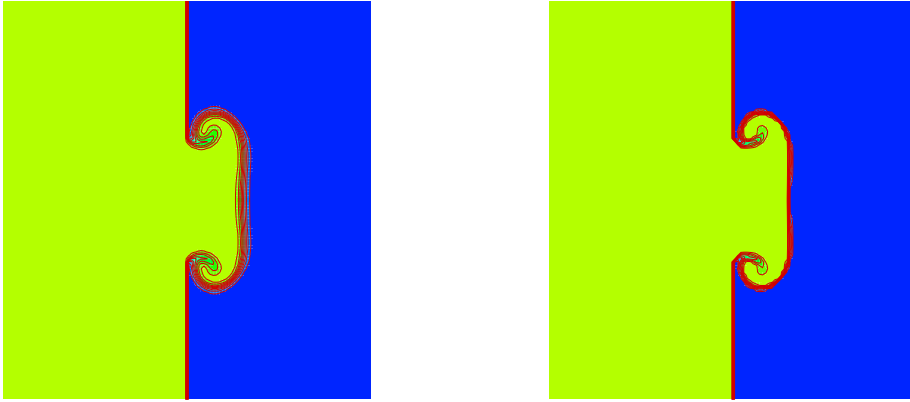


Figure 4.2: Example 4.2.1. 120×120 uniform mesh. Contours of T . Left: regular fifth order WENO; Right: anti-diffusive fifth order WENO.

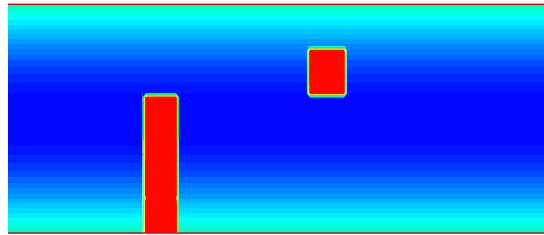


Figure 4.3: Example 4.2.2. Topography of the river bed. Red is the obstacle.

4.1 and 4.2 indicate excellent resolution of the location and concentration of the pollutant by our anti-diffusive scheme.

Example 4.2.2. River with obstacles. This is another test computed in [2], which is originally a test case in the code *TELEMAC* developed at EDF [8]. It is a river with obstacles in it. A simplified and scaled version of this problem we are computing here has the following setup: the computation domain is $(x, y) \in [0, 3] \times [0, 1]$ with a bottom topography

$$b(x, y) = \begin{cases} 0.4, & 0.75 < x < 0.95, 0 \leq y \leq 0.6 \\ 0.4, & 1.65 < x < 1.85, 0.6 < y < 0.8 \\ -0.2 \cos(\pi(y - 0.5)), & \text{otherwise} \end{cases} \quad (4.2)$$

which is depicted in Figure 4.3; the gravitational constant $g = 1.0$, $S = 0$, $u(x, y, 0) = 0.5$,

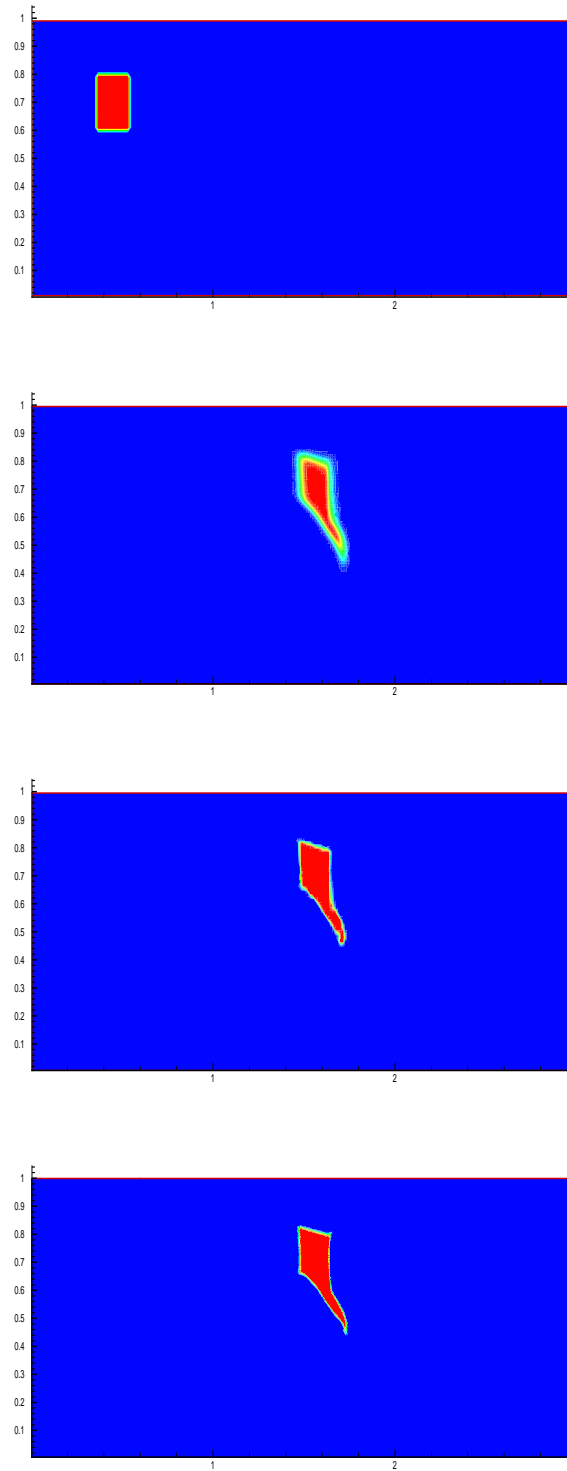


Figure 4.4: Example 4.2.2. 300×100 uniform mesh. Contours of T . Top: the initial pollutant; Second: pollutant obtained by the regular fifth order WENO; Third: pollutant obtained by the anti-diffusive fifth order WENO; Bottom: reference solution obtained by 1500×500 uniform mesh with regular fifth order WENO.

$v(x, y, 0) = 0$; the initial pollutant is given as

$$T(x, y, 0) = \begin{cases} 0.5, & 0.35 < x < 0.55, 0.6 \leq y \leq 0.8 \\ 0, & \text{otherwise} \end{cases} \quad (4.3)$$

and the scheme is run to $t = 2.0$. Again we observe sharp resolution of the location and concentration of the pollutant by our anti-diffusive scheme in Figure 4.4. Comparing with the reference solution at the bottom of Figure 4.4, which is computed with the regular WENO scheme with an extremely refined mesh and can be considered as an exact solution, the quality of the anti-diffusive WENO scheme is much better than that of the regular WENO scheme on the relatively coarse mesh with 300×100 points.

5. Concluding Remarks

The anti-diffusive flux corrections for high order finite difference scheme we explored in [18] is applied to the Saint-Venant shallow water model with transport of pollutant by a flow both in one dimension and two dimensions. We achieve high resolution of the location and concentration of the pollutant.

References

- [1] F. Bouchut, An antidiffusive entropy scheme for monotone scalar conservation law, *Journal of Scientific Computing*, **21** (2004), 1-30.
- [2] M.-O. Bristeau and B. Perthame, Transport of pollutant in shallow water using kinetic schemes, in CEMRACS 1999, ESAIM Proceedings 10, Soc. Math. Appl. Indust., Paris 1999, 9-21.
- [3] A. Chertock, A. Kurganov and G. Petrova, Finite-volume-particle methods for models for transport of pollutant in shallow water, *Journal of Scientific Computing*, to appear. Appeared on line (2006). DOI: 10.1007/s10915-005-9060-x.
- [4] B. Després and F. Lagoutière, Contact discontinuity capturing schemes for linear advection and compressible gas dynamics, *Journal of Scientific Computing*, **16** (2001), 479-524.
- [5] A. Harten, The artificial compression method for computation of shocks and contact discontinuities: III, *Mathematics of Computation*, **32** (1978), 363-389.
- [6] A. Harten, ENO schemes with subcell resolution, *Journal of Computational Physics*, **83** (1989), 148-184.
- [7] A. Harten, B. Engquist, S. Osher and S. Chakravathy, Uniformly high order accurate essentially non-oscillatory schemes, III, *Journal of Computational Physics*, **71** (1987), 231-303.
- [8] J.M. Hervouet, TELEMAC modelling system: an overview, *Hydrological Processes*, **14** (2000), 2209-2210.
- [9] G. Jiang and C.-W. Shu, Efficient implementation of weighted ENO schemes, *Journal of Computational Physics*, **126**(1996), 202-228.
- [10] X. Liu, S. Osher and T. Chan, Weighted essentially non-oscillatory schemes, *Journal of Computational Physics*, **115** (1994), 200-212.
- [11] P.L. Roe, Some contribution to the modelling of discontinuous flows, *Lectures in Applied Mathematics*, **22** (1985), 163-193.
- [12] C.-W. Shu, Essentially non-oscillatory and weighted essentially non-oscillatory schemes for hyperbolic conservation laws, in *Advanced Numerical Approximation of Nonlinear Hyperbolic Equations*, B. Cockburn, C. Johnson, C.-W. Shu and E. Tadmor (Editor: A. Quarteroni), Lecture Notes in Mathematics, volume 1697, Springer, 1998, pp.325-432.
- [13] C.-W. Shu, High order finite difference and finite volume WENO schemes and discontinuous Galerkin methods for CFD, *International Journal of Computational Fluid Dynamics*, **17** (2003), 107-118.

- [14] C.-W. Shu and S. Osher, Efficient implementation of essentially non-oscillatory shock-capturing schemes, *Journal of Computational Physics*, **77** (1988), 439-471.
- [15] C.-W. Shu and S. Osher, Efficient implementation of essentially non-oscillatory shock capturing schemes II, *Journal of Computational Physics*, **83** (1989), 32-78.
- [16] A.J.C. De Saint-Venant, Théorie du mouvement non-permanent des eaux, avec application aux crues des rivières et à l'introduction des marées dans leur lit, *Comptes rendus des séances de l'Académie des Sciences, Paris*, **73** (1871), 147-154.
- [17] P.K. Sweby, High resolution schemes using flux limiters for hyperbolic conservation laws, *SIAM Journal on Numerical Analysis*, **21** (1984), 995-1011.
- [18] Z. Xu and C.-W. Shu, Anti-diffusive flux corrections for high order finite difference WENO schemes, *Journal of Computational Physics*, **205** (2005), 458-485.
- [19] H. Yang, An artificial compression method for ENO schemes: the slope modification method, *Journal of Computational Physics*, **89** (1990), 125-160.